Frame-Synchronization for OFDM-Transmission with Sectorized Antenna Reception over Rapidly Fading Channels

Peter Klenner, Karl-Dirk Kammeyer

Department of Communications Engineering, University of Bremen
28359 Bremen, Germany
{klenner,kammeyer}@ant.uni-bremen.de

***Abstract*— OFDM is well-known for its ability to cope conveniently with severely frequency-selective channel conditions. However, the performance of OFDM is degraded if the channel is rapidly time-varying as well. Previously, sectorized receive antennas were shown to reduce the channel's effective Doppler spread. Thereby, rapid channel fluctuations are rendered into slow fluctuations. Hence, intercarrier-interference is avoided, and channel estimation and data detection are alleviated. In this paper we present a novel frame synchronization scheme to determine timing and frequency offsets for sectorized antenna reception.**

I. Introduction

OFDM's appeal stems from its ability to allow for low complexity equalization. This is achieved by increasing the symbol duration beyond the maximal channel delay and by choosing a suitable rectangular filter function. Thereby, the subcarriers become orthogonal, i.e., they are not interfering, and a multipath channel is basically transformed into a set of parallel flat-fading channels. An inherent assumption to uphold the subcarriers' orthogonality is the time-invariance of the channel which is violated for rapidly fading channels. Those will introduce intercarrier-interference.

In a previous paper, the authors demonstrated that sectorized receive antennas can effectively reduce the channel's time-selectivity prior to the receiver side FFT [1]. These sectorized receive antennas are directional and limit all possible angles of incidence to a finite range. Thus, it becomes possible to divide the Doppler spectrum with its full Doppler spread into subspectra with reduced Doppler spread. Hence, the channel impulse response of each sector is characterized by less time-selectivity than a comparable omnidirectional antenna and intercarrier interference is no longer an issue.

In the following, a timing and frequency synchronization scheme for sectorized reception is devised. Although it is eventually heuristic in nature, it is guided by a maximum-likelihood approach which is similar to [2]. However, its novelty lies in the exploitation of several OFDM symbols and of multiple receive antennas. Furthermore, our synchronization scheme is bandwidth-efficient in that it is based on the repetitive OFDM signal structure due to the cylic prefix, i.e., no additional training is required.

The remainder of the paper is organized as follows. In Section II we introduce our system model. Section III details our synchronization approach. Simulation results are presented in Section IV, and conclusions are drawn in Section V.

II. System Model

We consider a coherent and coded OFDM system with one transmit antenna and S sectorized receive antennas. Details about the latter are given in Section II-A. Forward error correction of the information bits is accomplished by a convolutional code of constraint length L_c and code rate $1/2$. The coded bits are randomly bit-interleaved and mapped to an M-ary PSK/QAM signal constellation. Since we are considering coherent reception the data symbols are multiplexed with pilot symbols yielding symbols $d(\nu, i)$ on the ν-th subcarrier in the i-th OFDM symbol. Throughout the paper we assume a rectangular pilot grid with pilot spacing Δ_f and Δ_t in frequency and time direction, respectively, i.e, the pilot positions in the OFDM time/frequency grid are integer multiples of Δ_f and Δ_t. The pilot symbols are drawn randomly and uniformly distributed from the same signal constellation as the data symbols. The receiver has perfect knowledge about them. After IFFT and prepending the cyclic prefix (CP) which consists of N_g symbols the OFDM transmit signal in complex equivalent baseband notation reads

$$x(k) = \frac{1}{\sqrt{N}} \sum_{i=-\infty}^{\infty} \sum_{\nu=0}^{N-1} d(\nu, i) \mathrm{e}^{\mathrm{j}2\pi\nu(k-iZ)/N} g(k - iZ)\,. \quad (1)$$

We defined the number of subcarriers to be N, $Z = N + N_\mathrm{g}$, as well as the rectangular filter function $g(k)$ which is 1 for $-N_\mathrm{g} \leq k < N$ and 0 otherwise. The receive signal at the s-th antenna reads

$$y(k, s) = \sum_{\ell=0}^{L-1} h(\ell, k, s) x(k - \ell - \theta) + n(k, s)\,, \quad (2)$$

where the additive white Gaussian noise with power σ_n^2 is denoted by $n(k, s)$ and the unknown timing offset by θ. It is assumed that θ is an integer value, deterministic and constant over the observation interval.

A. Sectorized Antennas

The purpose of sectorized antennas is the reduction of the channel's Doppler spread yielding impulse responses with reduced time-selectivity. We are modelling sectorized reception based on the wide-sense stationary and uncorrelated scattering (WSSUS) assumption which resembles a richly scattering and isotropic scenario. A channel impulse response for the s-th antenna in accord with the WSSUS assumption reads [3]

$$h(\ell,k,s)=\frac{1}{\sqrt{N_e}}\sum_{\mu=0}^{N_e-1}a(\mu,s)\mathrm{e}^{\mathrm{j}2\pi f_D(\mu,s)Tk}\delta(\ell-\ell(\mu,s)) \quad (3)$$

with delay index $0\le\ell<L$, time index k, sampling period T, and the length of the impulse response L. The N_e paths are characterized by their path amplitude $a(\mu,s)$, Doppler frequency $f_D(\mu,s)$ and delay $\ell(\mu,s)$.

Relative motion between transmitter and receiver leads to a Doppler shift of each impinging wave, an effect which is described by [4]

$$f_D(\mu,s)=f_{\mathrm{D,max}}\cos(\phi(\mu,s))\,. \quad (4)$$

Eq. (4) relates the maximum Doppler frequency $f_{\mathrm{D,max}}$ and the angle of incidence $\phi(s,\mu)$ of the μ-th path and s-th antenna to the resulting Doppler shift $f_D(\mu,s)$.

Omnidirectional reception is modelled by angles of incidence which are uniformly distributed in the interval $[0,2\pi]$. Then the famous U-shaped or Jakes' Doppler spectrum results. However, we are concerned with antennas which are sectorized and, hence, not omnidirectional. Their main benefit lies in the limitation of all possible angles of incidence to a finite range. Thus, they are exposed to a reduced Doppler spread leading to a less rapidly fading channel.

In the following we assume perfect sectorization, i.e., an impinging wave is assigned uniquely to an antenna according to its angle of incidence. For this case we configure the sectorized antennas such that the full Doppler spectrum is divided into equispaced subspectra [5]. This approach causes the same reduced Doppler spread in each antenna. In Tab. I the sector angles for $S=2,4,6,8$ sectors are given. It is assumed that the direction of motion coincides with the $0°$-direction. An example for the case $S=4$ is depicted in Fig. 1.

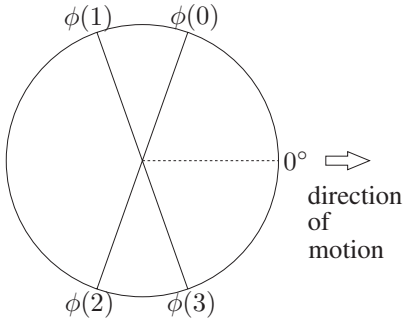

Fig. 1. Division of the horizontal receive plane into $S=4$ sectors

It depends on the scenario whether the sector alignment in practice is exactly as depicted in Fig. 1. For instance, if the sectorized antenna is mounted on top of a fast moving vehicle this can be easily fulfilled. In other cases it might be beneficial to choose a different sector configuration. In this paper we are mainly concerned with the former case.

TABLE I
SECTOR ANGLES FOR EQUAL DOPPLER PARTITIONING

S	$\phi(0)$	$\phi(1)$	$\phi(2)$	$\phi(3)$	$\phi(4)$	$\phi(5)$	$\phi(6)$	$\phi(7)$
2	90	270						
4	70.5	109.5	250.5	289.5				
6	60	90	120	240	270	300		
8	53.1	78.5	101.5	126.9	233.1	258.5	281.5	306.9

Each sectorized antenna experiences not only a reduced Doppler spread but also a Doppler shift [1], [5]. The Doppler shift needs to be compensated at the receiver prior to the FFT, otherwise it leads to leakage. The frequency $f_c(s)$ which is required for compensation is the mean frequency offset for each sector. The mean frequency follows from

$$f_c(s)=\int_{f_D(s)}^{f_D(s+1)}f_D\,p(f_D)\,\mathrm{d}f_D\,, \quad (5)$$

where $f_D(s)$ denotes the Doppler frequency corresponding to the angle of incidence $\phi(s)$, and $p(f_D)$ the probability density function (pdf) of the Doppler frequencies f_D. A simple approximation of (5) for uniformly distributed angles of incidence is given by [5]

$$f_c(s)\approx\begin{cases}f_{\mathrm{D,max}}\cos\left((\phi(s)/2\right), & s=0\\ -f_{\mathrm{D,max}}\sin\left((\phi(s)/2\right), & s=\frac{S}{2}\\ f_{\mathrm{D,max}}\cos((\phi(s)+\phi(s+1))/2), & \text{else}\,.\end{cases}$$

Compensation is achieved by

$$\tilde{y}(k,s)=\mathrm{e}^{-\mathrm{j}2\pi f_c(s)Tk}y(k,s)\,. \quad (6)$$

B. Correlations

The synchronization metric which we are about to derive depends on the correlation introduced by the channel. The WSSUS assumption leads to a separation of time and frequency correlation [3]. The channel correlation in time $\Theta(\kappa,s)$ which eventually influences the timing metric, is given by

$$\Theta(\kappa,s)=\mathrm{E}\left\{\mathrm{e}^{\mathrm{j}2\pi f_D(s)T\kappa}\right\}\,. \quad (7)$$

The mean is taken with respect to the probability density of the Doppler frequencies within the s-th sector. Thus, the autocorrelation function (ACF) of the receive signal in the s-th sector reads

$$r_{yy}(\kappa,s)=\mathrm{E}\{y(k,s)y^*(k+\kappa,s)\}=\sigma_x^2\Theta(\kappa,s)+\sigma_n^2\delta(\kappa)\,. \quad (8)$$

If the frequency offsets are known the timing correlation is given by

$$\Theta_c(\kappa,s)=\mathrm{E}\left\{\mathrm{e}^{\mathrm{j}2\pi(f_D(s)-f_c(s))T\kappa}\right\}\,. \quad (9)$$

The ACF of the frequency compensated signals reads

$$r_{\tilde{y}\tilde{y}}(\kappa,s)=\mathrm{E}\{\tilde{y}(k,s)\tilde{y}^*(k+\kappa,s)\}=\sigma_x^2\Theta_c(\kappa,s)+\sigma_n^2\delta(\kappa)\,. \quad (10)$$

III. Synchronization

Firstly, we are assembling the received symbols of all antennas at time instant k in the vector

$$\boldsymbol{y}(k) = [y(k,0), \cdots, y(k,S-1)]^{\mathrm{T}}. \tag{11}$$

Furthermore, let us define the set $\mathcal{T} = \{f_c(0), \cdots, f_c(S-1), \theta\}$, which contains the parameters to be determined. The antennas are spaced sufficiently close to safely assume the same timing offset for all of them. We maximize the conditional probability $p(\mathcal{T}|\{\boldsymbol{y}(k)|\forall k\})$, i.e, the probability of the frequency offsets $f_c(0), \cdots, f_c(S-1)$ and the timing offset θ conditioned on all received symbols. If we apply the mixed Bayes rule to the conditional probability we find the parameter set equivalently through

$$\mathcal{T} = \underset{\widetilde{\mathcal{T}}}{\operatorname{argmax}}\, p\left(\{\boldsymbol{y}(k)|\forall k\}\,|\,\widetilde{\mathcal{T}}\right). \tag{12}$$

Unlike [2] we utilize all OFDM symbols and all antennas to determine the timing and frequency offsets. The OFDM signal structure introduces correlations between certain symbols in a distance equal to the OFDM symbol length. The received symbols for the i-th OFDM symbol are thus collected in the vector

$$\boldsymbol{z}(i,\theta) = [\,\boldsymbol{y}(iZ+\theta-N_{\mathrm{g}})^{\mathrm{T}}, \cdots, \boldsymbol{y}(iZ+\theta+N-1)^{\mathrm{T}}\,]^{\mathrm{T}}. \tag{13}$$

Then exploitation of the statistical independence of the OFDM symbol allows for maximizing the log-likelihood function instead of (12)

$$\lambda_0(\widetilde{\mathcal{T}}) = \sum_{i=-\infty}^{\infty} \log p(\boldsymbol{z}(i,\tilde{\theta})). \tag{14}$$

We have dropped here the dependence on the hypotheses on the right hand side to avoid cluttering notation. The transmit signal (1) can be assumed to be Gaussian distributed if the number of subcarriers is sufficiently large which in practice usually is fulfilled. Hence, the receive signals (2) are jointly Gaussian and the vector $\boldsymbol{z}(i,\theta)$ is described by a normal distribution.

OFDM symbols are composed of a cyclic prefix and its replica in the core symbol. These portions are therefore correlated, whereas the remainder of the OFDM core symbols remains uncorrelated. With $\underline{k} = iZ + \theta + k$ we can write

$$p(\boldsymbol{z}(i,\theta)) = \prod_{k=-N_{\mathrm{g}}}^{-1} p(\boldsymbol{y}(\underline{k}), \boldsymbol{y}(\underline{k}+N)) \prod_{k=0}^{N-N_{\mathrm{g}}-1} p(\boldsymbol{y}(\underline{k})). \tag{15}$$

Note that (15) is the same likelihood metric as in [2]. However, in our approach it is only a partial metric to be used in (14). Substituting (15) in (14) and suitable expansion of numerator and denumerator leads to the metric ($\underline{k}' = iZ + \tilde{\theta} + k$)

$$\lambda_1(\widetilde{\mathcal{T}}) = \sum_{i=-\infty}^{\infty} \sum_{k=-N_{\mathrm{g}}}^{-1} \log \frac{p(\boldsymbol{y}(\underline{k}'), \boldsymbol{y}(\underline{k}'+N))}{p(\boldsymbol{y}(\underline{k}'))p(\boldsymbol{y}(\underline{k}'+N))}. \tag{16}$$

Eq. (16) utilizes all OFDM symbols and all antenna signals and can be considered optimal in this respect to derive the timing metric from. It contains the metric of [2] as a special case for one OFDM symbol and one antenna in AWGN. However, in this form (16) is impractical due to several reasons, which we will discuss in the following. This will direct us to practical implementations of (16).

The outer summation ranges over all OFDM symbols, i.e., $-\infty < i < \infty$, which is clearly not feasible. However, truncating the sum to a finite number of OFDM symbols renders the metric feasible ($\underline{k}'' = i'Z + \tilde{\theta} + k$)

$$\lambda_2(\widetilde{\mathcal{T}}(i)) = \sum_{i'=i-B}^{i} \sum_{k=-N_{\mathrm{g}}}^{-1} \log \frac{p(\boldsymbol{y}(\underline{k}''), \boldsymbol{y}(\underline{k}''+N))}{p(\boldsymbol{y}(\underline{k}''))p(\boldsymbol{y}(\underline{k}''+N))}. \tag{17}$$

Because of the truncation of the outer sum the timing offset will now be estimated for each OFDM symbol. Hence, it becomes time-varying and is now indexed by the OFDM symbol index i. However, this estimate is supported by $B+1$ OFDM symbols.

The application of (17) requires the specification of the pdfs. Those depend on the considered scenario. Since the receive signals (2) are antenna-wise uncorrelated, we have

$$\lambda_2(\widetilde{\mathcal{T}}(i)) = \sum_{s=0}^{S-1} \sum_{i'=i-B}^{i} \sum_{k=-N_{\mathrm{g}}}^{-1} \log \frac{p(y(\underline{k}'',s), y(\underline{k}''+N,s))}{p(y(\underline{k}'',s))p(y(\underline{k}''+N,s))}. \tag{18}$$

In its general form the summand of (18) is given in (19) on top of the next page. The last term of (19) depends on the autocorrelation function (8) of the receive signals. In the simulation results we will show the influence of different degrees of apriori knowledge at the receiver. For instance the AWGN and high SNR form of (19) is given by the Euclidean distance

$$\log \frac{p(y(k,s), y(k+N,s))}{p(y(k,s))p(y(k+N,s))} \propto -|y(k,s) - y(k+N,s)|^2. \tag{20}$$

A. Adaptation to multipath channels

Eq. (19) is valid only in the intersymbol-interference (ISI) free region of a cylic prefix. Hence, we are introducing a slight change in the inner sum of (18) to exclude those ISI-contaminated parts from the overall sum

$$\lambda_3(\widetilde{\mathcal{T}}(i)) = \sum_{s=0}^{S-1} \sum_{i'=i-B}^{i} \sum_{k=-N_s}^{-1} \log \frac{p(y(\underline{k}'',s), y(\underline{k}''+N,s))}{p(y(\underline{k}'',s))p(y(\underline{k}''+N,s))}. \tag{21}$$

In (18) all N_{g} samples of the CP are included, (21) is restricted to $N_s \leq N_{\mathrm{g}}$ samples. This approach leads to a timing plateau [6], i.e., a successive set of possible indicators for the timing offset. We found that a moving average filter of length $N_{\mathrm{g}} - N_s + 1$ is sufficient to concentrate the energy of the timing plateau into a triangular shape, whose peak is a reliable indicator of the timing offset. This specific length coincides with the size of the timing plateau for the AWGN case and was found through simulations to work just as well for the multipath case.

$$\log \frac{p(y(k,s),y(k,s))}{p(y(k,s))p(y(k+N,s))} \propto -|y(k,s)|^2 - |y(k+N,s)|^2 + 2r_{yy}(0,s)\mathrm{Re}\left\{\frac{y(k,s)y^*(k+N,s)}{r_{yy}(N,s)}\right\} \tag{19}$$

B. Detecting the timing offset and the frequency offsets

Eq. (21) can be seen as a form of preprocessing prior to the actual detection of the timing offset and the frequency offsets. To avoid an expensive exhaustive search over all hypotheses we resort to a suboptimal two-stage approach [2]. Initially, the timing offset is determined while the presence of the frequency offsets is completely disregarded. The detection itself is carried out based on a search window of OFDM symbol size, $N + N_\mathrm{g}$. Within this window the maximum of (21) is determined, whose position, $\hat{\theta}(i)$, is used as the timing offset for the current OFDM symbol. The search window is then advanced by $N+N_\mathrm{g}$ symbols. Simulation results indicate that the timing metric (20) which is appealing due to its low complexity works inferior compared to (19). Hence, in practice it is necessary to estimate the autocorrelation of the receive signals (8). With the timing offset estimated the frequency offsets are determined based on the last term on the right hand side of (19). Since the other terms are contributing only magnitude information, this is the only term containing phase information. Thus, we estimate the mean frequency for the s-th antenna and the i-th OFDM symbol by ($m = i'Z + \hat{\theta}(i) + k'$)

$$\hat{f}_c(i,s) = -\sum_{i'=i-B}^{i}\sum_{k'=-N_s}^{-1}\frac{\arg\{y(m,s)y^*(m+N,s)\}}{2\pi(B+1)T}. \tag{22}$$

Since an estimate of the frequency offsets is now available it becomes possible to compensate this frequency offsets prior to determining the timing offset. With respect to performing the timing synchronization based on (20) this approach is advisable since we are disregarding the presence of any frequeny offset for determining the timing offset. Hence, removing the frequency offsets will alleviate the estimation of the timing offset.

However, the maximum frequency offset which can be estimated is limited. Phase changes which are larger than π between symbols with OFDM symbol distance cause phase ambiguities. These can not be resolved. Ultimately, if a frequency offset estimate is required because we are lacking knowledge about the direction of the relative motion the maximum Doppler spread which can be compensated is also limited.

IV. Simulation Results

We present results for a coherent OFDM system with $N = 64$ subcarriers and a cyclic prefix of length $N_\mathrm{g} = 16$. A convolutional code with generator polynomial $(133, 171)_8$ and constraint length $L_c = 7$ is used for error protection. The pilot spacing is $\Delta_t = 2$ and $\Delta_f = 5$. Channel estimation is done based on linear interpolation. Firstly, the channel is estimated at the pilot positions by dividing through the pilot symbols. This is followed by linear interpolation first in frequency direction, then in time direction. We additionally assumed to have knowledge about the channel's power delay profile. Especially, it is necessary to know the center of gravity of the power delay profile, since our CP-based synchronisation scheme is biased towards it. In practice one needs to estimate it, otherwise it will lead to intersymbol interference since the timing offset leads to an FFT start within the core symbol. Another solution for this problem is to split the cyclic prefix into a cyclic pre- and a postfix. This retains the subcarrier's orthogonality and omits the error-prone estimation of the center of gravity of the channel's impulse response.

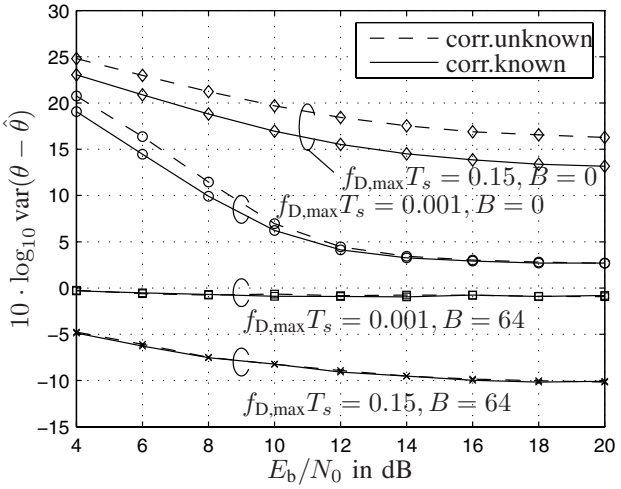

Fig. 2. Variance of the timing offset for the single transmit and receive antenna case, $L = 9$, $N_s = 6$

In Fig. 2 we consider the error variance of the detected timing offset vs. E_b/N_0 for the single transmit and receive antenna case. Two Doppler scenarios are chosen, representing slow ($f_{\mathrm{D,max}}T_s = 0.001$) and fast ($f_{\mathrm{D,max}}T_s = 0.15$) fluctuations. The parameter B controls the number of additional OFDM symbols which are used to detect the timing offset, i.e., for $B = 0$ only one OFDM symbol is used, whereas $B = 64$ exploits 64 additional OFDM symbols.

It is evident from Fig. 2 that the large Doppler frequency leads to a large variance of the detected timing offset, if only one OFDM symbol is used. Exploiting receiver side knowledge about the channel correlations serves for lowering the error variance. However, if we increase the number of additional OFDM symbols to $B = 64$ the error variance for the large Doppler case even becomes lower than for the slow fading case. Hence, we conclude that the inclusion of several OFDM symbols greatly enhances the reliability of CP-based synchronization, even for rapidly fading channels.

To strengthen this observation we consider the sectorized receive antenna case in Fig. 3. We have chosen $S = 8$ sectors, and frequency compensation is performed perfectly prior to timing synchronization. If the frequency offset is perfectly known, the error variance of the timing offset can be effectively decreased by enlarging B. This holds true for

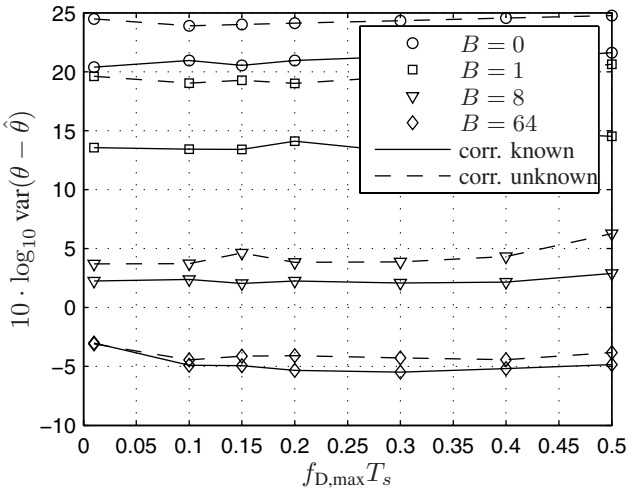

Fig. 3. Variance of the timing offset for the single transmit antenna and $S = 8$ receive antennas case, channel length $L = 9$, $N_s = 6$, $E_\mathrm{b}/N_0 = 5$ dB

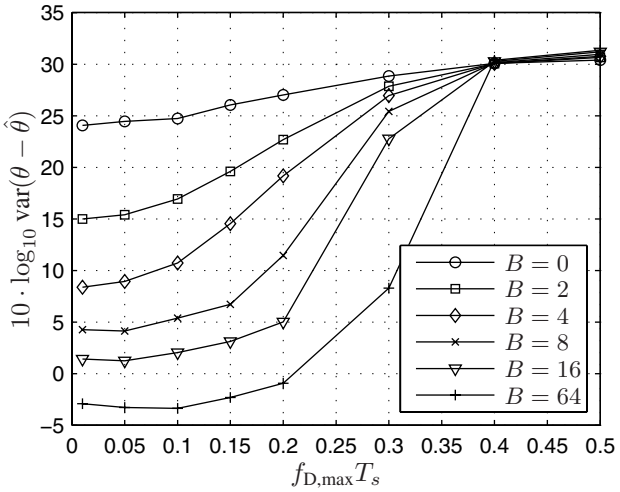

Fig. 4. Variance of the timing offset for the single transmit antenna and $S = 8$ receive antennas case without frequency compensation and neglecting channel correlations, channel length $L = 9$, $N_s = 6$, $E_\mathrm{b}/N_0 = 5$ dB

the metric which exploits the known correlation and for the metric (20) which completely disregards any correlations.

This behavior changes if the frequency offsets of the sectors are not compensated. For this non-compensated case Fig. 4 depicts the error variance of the timing offset vs. the normalized Doppler frequency $f_{\mathrm{D,max}} T_s$. Maximum Doppler frequencies beyond approximately 0.2 are deteriorating the detected timing offset, regardless of a larger number of supportive OFDM symbols.

For Fig. 5 we jointly estimated frequency and timing offsets like we discussed in Section III-B. We estimate the timing offset based on the frequency compensated receive signals. In turn the frequency offsets are estimated based on the detected timing offset, i.e., (22). The timing metric based on the known correlation clearly benefits from the frequency compensation. The SNR-loss due to imperfect synchronization is approximately 0.5 dB for $B = 64$. However, the timing

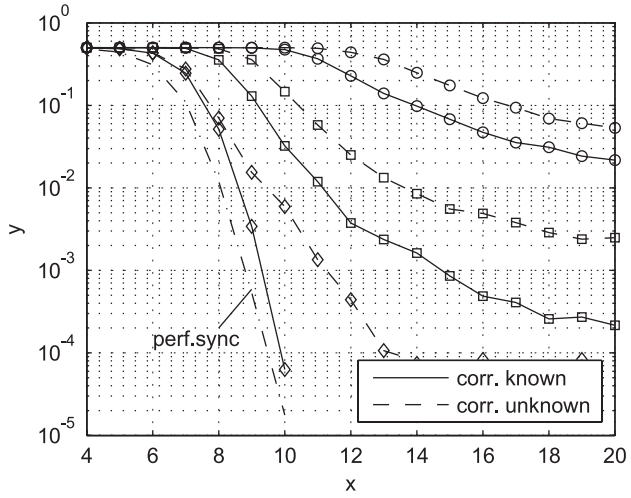

Fig. 5. BER vs E_b/N_0 for the single transmit antenna and $S = 8$ receive antennas case, $f_{\mathrm{D,max}} T_s = 0.2$ channel length $L = 9$, $N_s = 6$, legend: $B = 0$ (○), $B = 1$ (□), $B = 16$ (◇)

metric which disregards the correlation leads to an error-floor even for the case $B = 64$.

V. Conclusions

Sectorized antenna reception subdivides the Doppler spectrum into a number of subspectra with reduced Doppler spread. Thus each sector corresponds to an impulse response of reduced time-selectivity. Thereby intercarrier-interference is avoided, and the subcarriers stay orthogonal. A timing and frequency synchronisation for sectorized antenna reception was devised. It is cyclic prefix based, and introduces no additional need for training data. It is novel in that it exploits several OFDM symbols, all antennas and the channel correlations. We demonstrated that CP-based synchronisation does not deliver an accurate timing and frequency offset for rapidly fluctuating channels, if only one OFDM symbol is exploited. However, a feasible number of OFDM symbols does indeed increase the accuracy of the timing metric and allows for reliable data transmission, even under large Doppler influence. BER simulations revealed that it is necessary to estimate the channel correlations to ensure correct data transmission.

References

[1] P. Klenner and K. D. Kammeyer, "Doppler-Compensation for OFDM-Transmission by Sectorized Antenna Reception," in *Multi-Carrier Spread Spectrum 2007*, ser. Lecture Notes in Electrical Engineering. Springer, May 2007, pp. 237–246.

[2] J.-J. Beek, M. Sandell, and P. O. Börjesson, "ML Estimation of Time and Frequency Offset in OFDM Systems," *IEEE Transactions on Signal Processing*, vol. 48, pp. 1800–1805, July 1997.

[3] P. Höher, "A Statistical Discrete-Time Model for the WSSUS Multipath Channel," *IEEE Trans. on Vehicular Technology*, vol. 41, pp. 461–468, Nov. 1992.

[4] W. C. Jakes, *Microwave Mobile Communications*. IEEE Press, 1974.

[5] O. Norklit and R. G. Vaughan, "Angular Partitioning to Yield Equal Doppler Contributions," *IEEE Trans. on Vehicular Communications*, vol. 48, pp. 1437–1442, Sept. 1999.

[6] T.-M. Schmidl and D. C. Cox, "Robust Frequency and Timing Synchronization for OFDM," *IEEE Transactions on Communications*, vol. 45, no. 12, pp. 1613–1621, Dec. 1997.